Water Research 188 (2021) 116549

Contents lists available at ScienceDirect

Water Research

journal homepage: www.elsevier.com/locate/watres

DBP formation and toxicity alteration during UV/chlorine treatment of wastewater and the effects of ammonia and bromide

Zhechao Hua[a], Dan Li[b], Zihao Wu[a], Ding Wang[a,c], Yonglin Cui[a], Xiongfei Huang[a], Jingyun Fang[a,*], Taicheng An[d]

[a] Guangdong Provincial Key Laboratory of Environmental Pollution Control and Remediation Technology, School of Environmental Science and Engineering, Sun Yat-Sen University, Guangzhou 510275, China
[b] Department of Environmental Science & Engineering, Fudan University, Shanghai 200433, China
[c] Independent researcher, 25 Tuscany Springs Terr NW, Calgary, AB T3L 2V2, Canada
[d] Guangdong Key Laboratory of Environmental Catalysis and Health Risk Control, School of Environmental Science and Engineering, Institute of Environmental Health and Pollution Control, Guangdong University of Technology, Guangzhou 510006, China

ARTICLE INFO

Article history:
Received 16 July 2020
Revised 16 October 2020
Accepted 21 October 2020
Available online 22 October 2020

Keywords:
UV/chlorine
Disinfection by-products
Toxicity
Ammonia
Bromide
Wastewater

ABSTRACT

The UV/chlorine process is efficient for the abatement of micropollutants; yet, the formation of disinfection by-products (DBPs) and the toxicity can be altered during the treatment. This study investigated effluent organic matter characterization, DBP formation and toxicity alteration after the UV/chlorine treatment of wastewater; particularly, typical water matrix components in wastewater, namely, ammonia and bromide, were studied. The raw wastewater contained low levels of ammonia (3 μM) and bromide (0.5 μM). The UV/chlorine treatment efficiently eliminated 90 – 94% of fluorescent components. Compared with chlorination alone, a 20 min UV/chlorine treatment increased the formation of trihalomethanes (THMs), haloacetic acids (HAAs), chloral hydrate (CH), haloacetonitriles (HANs), trichloronitromethane (TCNM) and haloacetamides (HAcAms) by 90 – 508%. In post-chlorination after the UV/chlorine treatment, the formation of CH, HANs, TCNM and HAcAms increased by 77 – 274%, whereas the formation of both THMs and HAAs increased slightly by 11%. Meanwhile, the calculated cytotoxicity and genotoxicity of DBPs increased considerably after the UV/chlorine treatment and in post-chlorination, primarily due to the increased formation of HAAs and nitrogenous DBPs (N-DBPs). However, the acute toxicity of the wastewater to *Vibrio fischeri* and genotoxicity determined by the *umu* test decreased by 19% and 76%, respectively, after the 20 min UV/chlorine treatment. An additional 200 μM ammonia decreased the formation of all detected DBPs during the UV/chlorine treatment and 24 h post-chlorination, except that TCNM formation increased by 11% during post-chlorination. The acute toxicity of wastewater spiked with 200 μM ammonia was 32% lower than that of raw wastewater after the UV/chlorine treatment, but the genotoxicity was 58% higher. The addition of 1 mg/L bromide to the UV/chlorine process dramatically increased the formation of brominated DBPs and the overall calculated cytotoxicity and genotoxicity of DBPs. However, the acute toxicity and genotoxicity of the wastewater decreased by 7% and 100%, respectively, when bromide was added to the UV/chlorine treatment. This study illuminated that UV/chlorine treatment can decrease acute and geno- toxicities of wastewater efficiently.

1. Introduction

UV/chlorine treatment is an emerging advanced oxidation process (AOP) that has already been applied in water and wastewater treatment and potable water reuse (Guo et al., 2018; Chuang et al., 2019). Its efficiency in micropollutant degradation and its lower energy consumption than UV/H_2O_2 treatment are desirable in wastewater treatment (Sichel et al., 2011; Guo et al., 2018). The formed Reactive chlorine species (RCS), such as $Cl^{\cdot}$, $ClO^{\cdot}$ and $Cl_2^{\cdot-}$, have been shown to have a higher reactivity towards target compounds with electron-rich moieties than hydroxyl radicals ($HO^{\cdot}$) (Fang et al., 2014; Guo et al., 2017; Hua et al., 2019a).

The formation of disinfection by-products (DBPs) is one of the major concerns when considering the application of UV/chlorine in water treatment, because RCS are formed and expected to react with organic matter (Remucal and Manley, 2016). Compared with chlorination alone, UV/chlorine treatment in full-scale drink-

* Corresponding author.
E-mail address: fangjy3@mail.sysu.edu.cn (J. Fang).

https://doi.org/10.1016/j.watres.2020.116549
0043-1354/

Nomenclature

3,5-DCP	3,5-dichlorophenol
4-NQO	4-nitroquinoline-N-oxide
AOP	Advanced oxidation process
AOX	Adsorbable organic halogen
BCAA	Bromochloroacetic acid
BCAcAm	Bromochloroacetamide
BCAN	Bromochloroacetonitrile
BDCAA	Bromodichloroacetic acid
BDCAcAm	Bromodichloroacetamide
BDCM	Bromodichloromethane
BIF	Bromine incorporation factor
CDBAA	Chlorodibromoacetic acid
CH	Chloral hydrate
CHO	Chinese hamster ovary
DBAA	Dibromoacetic acid
DBAcAm	Dibromoacetamide
DBAN	Dibromoacetonitrile
DBCM	Dibromochloromethane
DBPs	Disinfection by-products
DCAA	Dichloroacetic acid
DCAcAm	Dichloroacetamide
DCAN	Dichloroacetonitrile
DOM	Dissolved organic matter
ECD	Electron capture detector
EEM	Excitation emission matrix
EfOM	Effluent organic matter
HA	Humic acid
HAAs	Haloacetic acids
HAcAms	Haloacetamides
HANs	Haloacetonitriles
HLB	Hydrophile lipophilic balance
$HO^{\cdot}$	Hydroxyl radicals
HPLC	High performance liquid chromatography
LC_{50}	Lethal concentration to 50%
MBAA	Bromoacetic acid
MTBE	Methyl tert-butyl ether
MW	Molecular weight
N-DBPs	Nitrogenous DBPs
NOM	Natural organic matter
PARAFAC	Parallel factor
RBS	Reactive bromine species
RCS	Reactive chlorine species
RNS	Reactive nitrogen species
SPE	Solid-phase extraction
TBAA	Tribromoacetic acid
TBM	Tribromomethane
TCAA	Trichloroacetic acid
TCAcAm	Trichloroacetamide
TCAN	Trichloroacetonitrile
TCM	Trichloromethane
TCNM	Trichloronitromethane
THMs	Trihalomethanes
TOC	Total organic carbon
WWTP	Wastewater treatment plant

ing water treatment plants (Wang et al., 2015; Wang et al., 2019) and natural organic matter (NOM) solutions (Wang et al., 2017; Gao et al., 2019) was reported to significantly increase the formation of trihalomethanes (THMs), haloacetic acids (HAAs) and adsorbable organic halogen (AOX), whereas a slight decrease in trichloromethane (TCM) and trichloroacetic acid (TCAA) formation in a humic acid (HA) solution was also observed (Li et al., 2016). The discrepancy could be caused by different experimental conditions and water matrices. Compared with NOM in drinking water sources, wastewater effluent organic matter (EfOM) contains more hydrophilic substances (Ma et al., 2001), which are more reactive towards chlorine. The quantities of dissolved organic matter (DOM) in wastewater effluents are always higher than those in drinking water sources, and the components in wastewater are much more complex. Therefore, DBP formation after the UV/chlorine treatment of wastewater requires further investigation.

Toxicity alteration during water treatment is linked to the transformation products of DOM and water matrices. Many indicators, such as the acute toxicity to luminous bacteria (*Vibrio fischeri*) (Parvez et al., 2006), genotoxicity to genetically modified strains (*S. typhimurium*) determined by the in vitro *umu* test (Reifferscheid and Heil, 1996), and chronic cytotoxicity and acute genotoxicity to Chinese hamster ovary (CHO) cells (Plewa et al., 2004), can represent the toxicity of water samples. The acute toxicity to *Vibrio fischeri* decreased when the UV/chlorine process was applied to the abatement of trimethoprim (Wu et al., 2016) and naphthenic acid (Shu et al., 2014). The genotoxicity and cytotoxicity to CHO cells were observed to decrease significantly when UV photolysis and chlorine were combined in a drinking water plant and applied to reclaimed water (Plewa et al., 2012; Lv et al., 2017). The cytotoxicity of NOM increased after UV/chlorine treatment and was higher than that after chlorination alone (Wang et al., 2017). Hence, toxicity alteration after the UV/chlorine treatment of wastewater must be investigated further.

In addition, the water matrices of wastewater are more complex than those of drinking water. For example, the concentrations of ammonia and bromide are relatively higher in wastewater, which can significantly affect the chlorine and radical chemistry in UV/chlorine systems. Ammonia can quickly transform chlorine into chloramine, which can increase the formation of nitrogenous DBPs (N-DBPs) (Huang et al., 2017) with higher toxicity than regulated DBPs (e.g., THMs and HAAs) (Muellner et al., 2007). Also, the UV/chlorine process converts to the UV/chloramine process, which has a significantly different chemistry from the former. The UV/monochloramine (NH_2Cl) process primarily produces $Cl^{\cdot}$ and $NH_2^{\cdot}$. Then, $Cl^{\cdot}$ reacts with H_2O/OH^- and chloride to generate $HO^{\cdot}$ and $Cl_2^{\cdot-}$, respectively, and $NH_2^{\cdot}$ can be transformed into other RNS such as $NO^{\cdot}$ and $NO_2^{\cdot}$ in the presence of dissolved oxygen (Li and Blatchley III, 2009; Wu et al., 2019). The steady-state concentrations of $HO^{\cdot}$ and $Cl^{\cdot}$ in UV/NH_2Cl under neutral conditions were higher than those in UV/chlorine (Chuang et al., 2017). The involvement of $NO^{\cdot}$ and $NO_2^{\cdot}$ can increase the formation of trichloronitromethane (TCNM) during the UV/NH_2Cl treatment of ibuprofen (Wu et al., 2019). However, DBP formation and toxicity alteration after the UV/chlorine treatment of wastewater in the presence of a high concentration ammonia are largely unstudied.

The concentration of bromide can reach 4.1 mg/L in a surface water (Magazinovic et al., 2004) and over 1 mg/L in wastewater effluents (Soltermann et al., 2016). The presence of bromide increases the formation of brominated DBPs, which are more toxic than chlorinated DBPs, during chlorination (Sun et al., 2009). However, the presence of bromide significantly decreases the genotoxicity of wastewater (Wu et al., 2010). In the UV/chlorine process, bromide quickly forms free bromine, which is then photolysed by UV radiation to produce bromine-containing species such as $Br^{\cdot}$ and $Br_2^{\cdot-}$ (Wu et al., 2017b; Guo et al., 2020). The presence of bromide in the UV/chlorine process can significantly promote the degradation of some micropollutants while inhibiting that of others (Wu et al., 2017b; Cheng et al., 2018). Compared with the medium pressure UV photolysis of chlorine in the absence of bromide, that in the presence of bromide significantly increased the formation of total organic bromine in a NOM solution, but decreased the formation of AOX (Zhao et al., 2011). Bromide in the

Table 1
Parameters of secondary wastewater effluent.

pH	DOC (mg/L)	NH_4^+ (mgN/L)	Cl^- (mg/L)	Br^- (μg/L)	NO_3^- (mgN/L)	NO_2^- (mgN/L)	SO_4^{2-} (mg/L)	Alkalinity ($CaCO_3$, mg/L)
7.7	4.5	0.04	36.9	40	2.7	0.01	61.4	90.4

UV/chlorine process can decrease the formation of THMs, HAAs and haloacetonitriles (HANs) in a HA solution at a UV fluence rate of 1200 mJ/cm^2 (Gao et al., 2020). However, studies of the effects of bromide on specific DBP formation in wastewater and toxicity alteration of wastewater during UV/chlorine treatment are rare.

The purposes of this study were to (1) investigate the alteration of EfOM characteristics after UV/chlorine treatment, (2) evaluate DBP formation in the UV/chlorine process and post-chlorination, (3) assess the calculated cytotoxicity and genotoxicity of DBPs and the acute toxicity and genotoxicity of wastewater after UV/chlorine treatment, and (4) explore the effects of high concentrations of ammonia and bromide in the UV/chlorine process on EfOM characteristics, DBP formation and toxicity alteration.

2. Materials and methods

2.1. Materials

All solutions were prepared from reagent-grade chemicals and ultrapure water (18.2 MΩ/cm) purified by a Milli-Q system. Sodium hypochlorite (NaOCl, 4.00-4.99%) and ascorbic acid were purchased from Sigma-Aldrich (St. Louis, MO, USA). Sodium bromide, sodium sulfite and ammonium sulfate were obtained from Sinopharm Chemical Reagent Co., Ltd. (Shanghai, China). High-performance liquid chromatography (HPLC) grade methyl *tert*-butyl ether (MTBE) was purchased from Thermo Fisher (USA). A ~3000 mg/L free chlorine stock solution was diluted from a 4.00-4.99% NaOCl solution and periodically standardized by DPD/FAS titration (APHA-AWWA-WEF, 2012). A secondary wastewater effluent sample was obtained from the Datansha wastewater treatment plant (WWTP) in Guangdong Province, China, and then filtered through glass fibre filters (Whatman GF/F). The parameters of the WWTP effluent are listed in Table 1.

2.2. Experimental procedures

The photochemical experiments were performed in a 700 mL cylindrical borosilicate glass reactor with a low-pressure mercury lamp (254 nm, GPH 212T5L/4, 10 W, Heraeus) contained in a quartz tube in the centre. A thermostat (THD-0515, Tianheng, China) was used to control the solution temperature at 25 ± 0.2 °C. The photon flux (I_0) entering the solution was determined to be 0.57 μEinstein s^{-1} using iodide/iodate chemical actinometry (Bolton et al., 2011). The effective optical path length (L) was determined to be 3.32 cm by measuring the H_2O_2 photolysis kinetics (Baxendale and Wilson, 1957). The corresponding average UV fluence rate (Ep^0) was 1.27 mW cm^{-2}.

A 700 mL wastewater effluent was dosed with 200 μM free chlorine or H_2O_2 and simultaneously exposed to UV light for 20 min. Samples were collected and divided into five portions. The first portion (10 mL) was analysed to determine the residual chlorine or H_2O_2. The second and third portions (40 mL) were quenched by ascorbic acid to analyse the volatile DBPs and HAAs, respectively. The fourth portion (20 mL) was quenched by sodium sulfite for the analyses of fluorescence spectroscopy and UV absorbance. The fifth portion (550 mL) was quenched by sodium sulfite to analyse the acute toxicity and genotoxicity, which involved the acidification to pH 2 with 10% dilute sulfuric acid (v/v) and solid-phase extraction (SPE) using hydrophile lipophilic balance (HLB) cartridges (200 mg, 6 mL, CNW). Control tests were conducted by applying UV or chlorine alone under parallel conditions. To explore the effects of high concentrations of ammonia and bromide during UV/chlorine treatment, 200 μM ammonia or 1 mg/L bromide was spiked into wastewater before the UV/chlorine treatment. To investigate the DBP formation potential during post-chlorination, samples subjected to UV/chlorine, UV/H_2O_2, UV, and chlorination treatments for 20 min were chlorinated in headspace-free amber bottles in the dark at 25°C for 24 h, and the residual chlorine was greater than 1 mg/L . The samples treated by the UV/H_2O_2 process were spiked with aliquots of chlorine to remove residual H_2O_2 and ensure a chlorine dosage of 200 μM before 24 h chlorination. All experiments were performed at least twice, and the error bars in the figures represent the maximum and minimum of the replicates. The significance of observed differences was evaluated by using student's t test to calculate P values and $P < 0.05$ was considered statistically significant.

2.3. Analytical methods

Chlorine concentrations were determined by the DPD colorimetric method (APHA-AWWA-WEF, 2012). The volatile DBPs, including THMs of TCM, bromodichloromethane (BDCM), dibromochloromethane (DBCM) and tribromomethane (TBM), CH, HANs of dichloroacetonitrile (DCAN), trichloroacetonitrile (TCAN), bromochloroacetonitrile (BCAN) and dibromoacetonitrile (DBAN), TCNM and haloacetamides (HAcAms) of dichloroacetamide (DCAcAm), trichloroacetamide (TCAcAm), bromochloroacetamide (BCAcAm), dibromoacetamide (DBAcAm) and bromodichloroacetamide (BDCAcAm) were analysed based on USEPA Method 551.1 (USEPA, 1995) and HAAs of dichloroacetic acid (DCAA), TCAA, bromoacetic acid (MBAA), bromochloroacetic acid (BCAA), bromodichloroacetic acid (BDCAA), dibromoacetic acid (DBAA), chlorodibromoacetic acid (CDBAA) and tribromoacetic acid (TBAA) were analysed based on USEPA Method 552.3 (USEPA, 2003), using a gas chromatograph (Agilent 7890A, USA) coupled with an electron capture detector (ECD). The pH was measured with a pH meter (Mettler Toledo, FE20). The dissolved organic carbon (DOC) was measured using a total organic carbon (TOC) analyser (Shimadzu TOC-V_{CPH}, Japan). The concentrations of Cl^-, Br^-, NO_3^-, NO_2^- and SO_4^{2-} in the wastewater were measured by an ion chromatography system (ICS-900, Dionex) equipped with a conductivity detector. The concentration of ammonia was determined by Nessler's reagent spectrophotometry, while alkalinity was measured by titration method with methyl orange as an indicator. The UV absorbance was measured by a UV-Vis spectrophotometer (TU-1900, Persee, China). Fluorescence excitation emission matrix (EEM) spectra were measured using a fluorescence spectrophotometer (HORIBA, Aqualog-UV-800). The collected EEMs were further examined by parallel factor (PARAFAC) analysis to extract various fluorescence components in MATLAB (Murphy et al., 2013).

The cytotoxicity and genotoxicity of the DBPs were calculated by dividing the concentrations of the detected DBPs by their lethal concentration to 50% (LC_{50}) values and 50% Tail DNA (or mid-point of Tail moment), respectively (Chuang et al., 2019), which were obtained from the toxicity data reported by Wagner and Plewa (2017) determined using CHO cells (Table S2). The total cyto-

toxicity and genotoxicity of the DBPs were calculated by summing the values for each DBP to evaluate the toxicity alteration induced by the DBPs during different treatments.

The acute toxicity was analysed using a LUMIStox toxicity analyser (HACH, USA) and *Vibrio fischeri* strains (Wu et al., 2016). After 30 min reaction, the luminescence intensities of the samples were measured and reported as the luminescence inhibition (%). The acute toxicity was reported as the equivalent concentration of 3,5-dichlorophenol (3,5-DCP) (mg 3,5-DCP/L). The genotoxicity was analysed by SOS/*umu* tests using *Salmonella typhimurium* TA1535/pSK1002 according to a previous study (Wu et al., 2017a). The genotoxicity was expressed as the equivalent concentration of 4-nitroquinoline-N-oxide (4-NQO) (μg 4-NQO/L). It was noted that nearly all the volatile DBPs and inorganic DBPs were lost due to SPE extraction and nitrogen dry-up (Zhong et al., 2019). Therefore, the acute toxicity and genotoxicity were the toxicities of organic extracts, including EfOM and non-volatile organic transformation products, in the wastewater.

2.4. Kinetic model simulation

The steady-state concentrations of the reactive species in the UV/chlorine processes were simulated by a kinetic model using Kintecus v4.55 (Ianni, 2015) according to previous studies (Guo et al., 2018; Wu et al., 2019). Ammonia- and bromine-related reactions were considered when modelling the concentrations of radicals in wastewater. Details of the reactions employed in the model are listed in Table S1.

3. Results and discussion

3.1. Impacts of UV/chlorine treatment on EfOM characterization, DBP formation and toxicity alteration

3.1.1. EfOM characterization in UV/chlorine-treated wastewater

Fig. 1 shows the degradation of different fluorescent components and the alteration of the UV absorbance of the wastewater at 254 nm (UVA_{254}) after UV photolysis, chlorination, and the UV/chlorine treatment. The EEM spectra were divided into three regions according to the PARAFAC analysis. C1, C2 and C3 exhibited maximum fluorescence intensities at Ex/Em = 325/400 nm, 240/460 nm and 280/320 nm, respectively (Fig. S1), which were attributed to humic acid-, fulvic acid- and protein-like components,

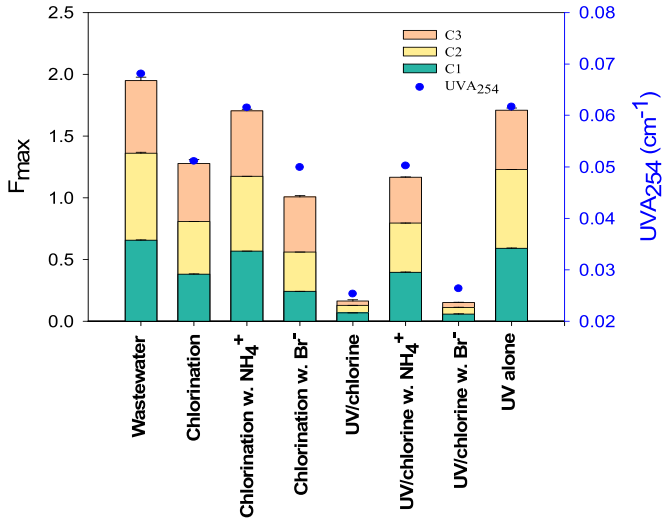

Fig. 1. PARAFAC fluorescent components and UVA_{254} of wastewater treated by UV, chlorination, and UV/chlorine with or without additional ammonia and bromide. Conditions: [chlorine] = 200 μM, [NH_4^+] = 200 μM, [Br^-] = 1 mg/L, pH = 7.7.

respectively (Chen et al., 2003). UV photolysis and chlorination alone could degrade 9 – 10% and 20 – 42%, respectively, of the diverse fluorescent components in the wastewater. The UV/chlorine treatment improved the removal efficiency of fluorescent components to 90 – 94%.

Most of the components in the wastewater were resistant to UV photolysis. Chlorination tended to react with humic substances, such as humic acid and fulvic acid (C1 and C2) (Korshin et al., 1999). The reactive species formed in the UV/chlorine process, such as $HO^{\cdot}$ and RCS, led to decreases of more than 90% in diverse components in the wastewater ($P < 0.05$). These results were consistent with those of a previous study, which reported that UV/chlorine treatment accelerated the destruction of chromophoric components (Pisarenko et al., 2013). During UV/H_2O_2 treatment, C1 and C2 in the wastewater were degraded by 47 – 48%, and C3 was degraded by 77% after 20 min at the same dosage of oxidant (200 μM) (Fig. S2), indicating that $HO^{\cdot}$ preferred to consume protein-like components in the wastewater. The rate constant of EfOM with $HO^{\cdot}$ was 3.3×10^4 $(mg\ L^{-1})^{-1}\ s^{-1}$ (Yang et al., 2016). The steady state concentrations of $HO^{\cdot}$ determined by the kinetic model were 6.78×10^{-14} M and 5.64×10^{-13} M in the UV/chlorine and UV/H_2O_2 processes, respectively. The steady-state concentrations of $Cl^{\cdot}$, $ClO^{\cdot}$ and $Cl_2^{\cdot-}$ were 1.01×10^{-14} M, 1.77×10^{-12} M and 7.79×10^{-13} M, respectively, in the UV/chlorine process. $Cl^{\cdot}$ and $ClO^{\cdot}$ reacted with EfOM with rate constants of 1.3×10^4 and 1.8×10^4 $(mg\ L^{-1})^{-1}\ s^{-1}$, respectively (Guo et al., 2018), while the rate constant of $Cl_2^{\cdot-}$ with EfOM was estimated to be 200 $(mg\ L^{-1})^{-1}\ s^{-1}$ (Brigante et al., 2014). In addition, SO_4^{2-} does not affect the radical chemistry in the UV/chlorine process, while alkalinity components of HCO_3^-/CO_3^{2-} can react with $HO^{\cdot}$ and RCS to generate $CO_3^{\cdot-}$ with the concentration of 9.66×10^{-11} M. The rate constant of EfOM with $CO_3^{\cdot-}$ was reported to be 76 $(mg\ L^{-1})^{-1}\ s^{-1}$ (Yan et al., 2019). Then the transformation rates of EfOM by $HO^{\cdot}$, $Cl^{\cdot}$, $Cl_2^{\cdot-}$, $ClO^{\cdot}$ and $CO_3^{\cdot-}$ were estimated to be $2.7 \times 10^{-5}\ s^{-1}$, $1.6 \times 10^{-6}\ s^{-1}$, $1.9 \times 10^{-6}\ s^{-1}$, $3.8 \times 10^{-4}\ s^{-1}$ and $8.8 \times 10^{-5}\ s^{-1}$, respectively. Therefore, $ClO^{\cdot}$ played a more important role in degrading diverse fluorescent components of wastewater in the UV/chlorine process.

After UV photolysis and chlorination alone, UVA_{254} decreased by 9% and 25%, respectively, whereas it decreased by 62% after the UV/chlorine treatment. UVA_{254} represents the aromaticity and/or hydrophobicity of DOM (Hwang et al., 2002). Reactive species could be responsible for the significant decrease in UVA_{254} in the UV/chlorine process. In the UV/H_2O_2 process, UVA_{254} only decreased by 18% (Fig. S2), which was consistent with the results of a previous study, in which a much higher decrease in the UVA_{254} of wastewater was observed after UV/chlorine treatment than after UV/H_2O_2 treatment (Miklos et al., 2019). Chlorination and RCS were likely the causes of the higher efficiency in decreasing the aromaticity.

3.1.2. DBP formation in UV/chlorine-treated wastewater

Fig. 2 shows the DBP formation during 20 min treatments by UV, chlorination, and UV/chlorine and 24 h post-chlorination. Compared to chlorination alone, the 20 min UV/chlorine treatment significantly promoted the formation of detected DBPs by 90 – 508% ($P < 0.05$). RCS is more reactive towards organic compounds than chlorine (Guo et al., 2017), resulting in more reaction sites. $Cl^{\cdot}$ can directly form chlorinated transformation products via radical addition (Lei et al., 2019; Bulman and Remucal, 2020), which could explain the enhanced DBP formation during the UV/chlorine treatment.

During 24 h post-chlorination after the 20 min UV/chlorine treatment, the regulated DBPs of THMs and HAAs increased slightly by 11% relative to those obtained by chlorination alone ($P < 0.05$), whereas the formation of unregulated DBPs, such as CH,

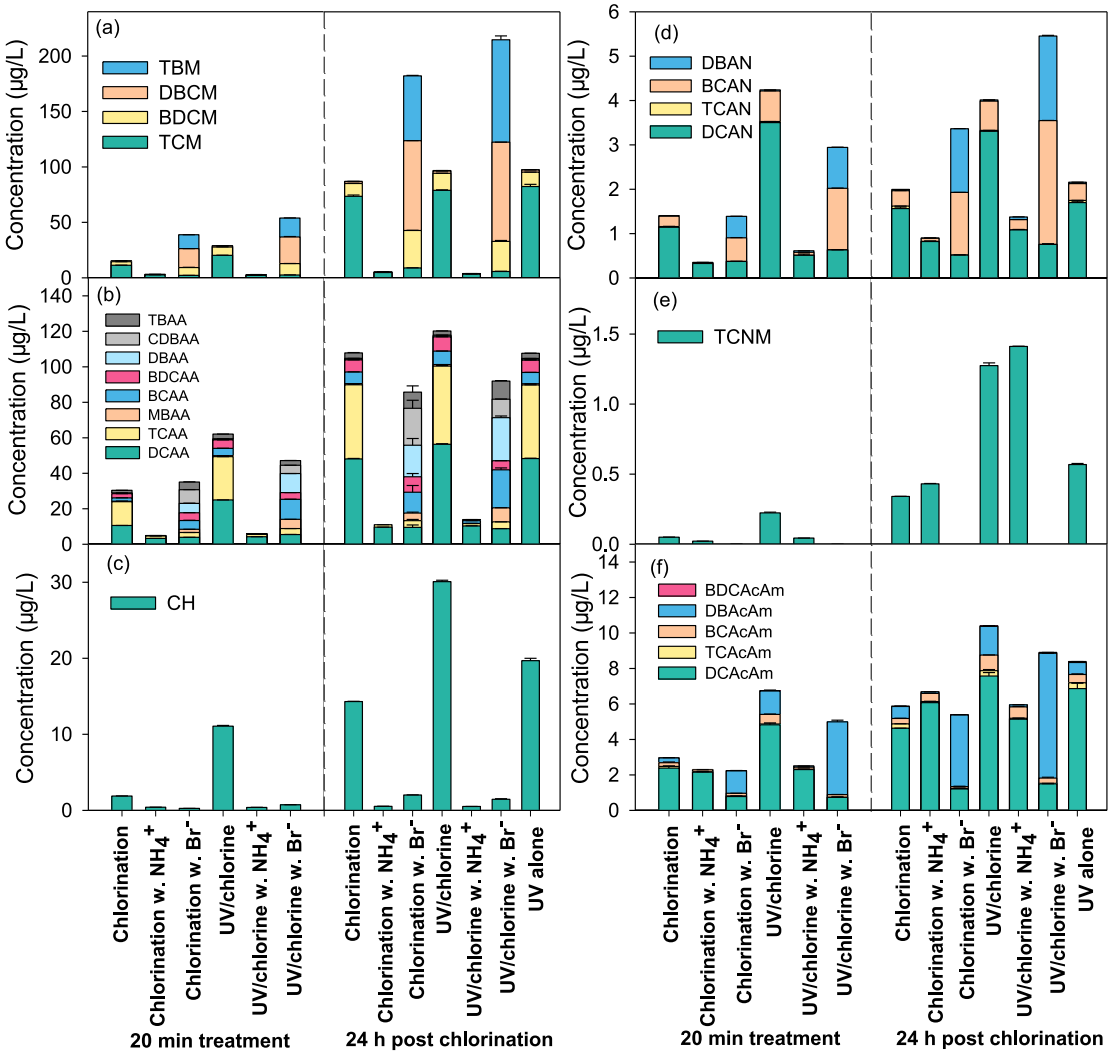

Fig. 2. DBP formation during UV, chlorination and UV/chlorine treatments with or without additional ammonia and bromide, and 24 h post chlorination of wastewater. Conditions: [chlorine] = 200 μM, [NH_4^+] = 200 μM, [Br^-] = 1 mg/L, pH = 7.7.

HANs, TCNM, and HAcAms, increased significantly by 77 – 274% ($P < 0.05$). In addition, UV photolysis of the wastewater increased the formation of CH, TCNM and HAcAms by 38%, 67% and 43%, respectively ($P < 0.05$), after 24 h post-chlorination.

The involvement of $HO^{\cdot}$ and RCS can alter the properties of organic matter, producing more intermediates that readily react with chlorine to form more DBPs in post-chlorination (Wang et al., 2015; Gao et al., 2020). $Cl^{\cdot}$ can react with organic substances via hydrogen abstraction, electron transfer and addition, whereas the reaction mechanisms of $ClO^{\cdot}$ and $Cl_2^{\cdot-}$ are mainly electron transfer (Alfassi et al., 1988; Lei et al., 2019); thus, RCS accelerated the formation of chlorinated products and DBPs (Bulman and Remucal, 2020). Meanwhile, $HO^{\cdot}$ and RCS could activate some precursors in wastewater, which readily reacted with chlorine in post-chlorination. $HO^{\cdot}$ increased the formation of aldehydes from organic substances (Xie et al., 2015), providing CH precursors during post-chlorination. On the other hand, the reduced aromaticity could decrease the formation potential of THMs and HAAs (Lamsal et al., 2011). DOC decreased by 15% during the UV/chlorine treatment primarily via radical oxidation (Fig. S3), resulting in the decrease of some DBP precursors. Therefore, the formation of THMs and HAAs increased modestly after the UV/chlorine treatment compared with chlorination alone.

In terms of N-DBPs, the UV/chlorine treatment accelerated the formation of HANs in a short period Wang et al., 2015). The base hydrolysis of HANs can increase the formation of HAcAms (Reckhow et al., 2001). Both $HO^{\cdot}$ and RCS can transform the amine moieties of organic compounds into nitro moieties (Deng et al., 2014; Hua et al., 2019b), leading to increased TCNM formation. The formation of N-DBPs in post-chlorination after the UV/chlorine treatment was 77 – 101% higher than that after the UV/H_2O_2 treatment (Fig. S4), indicating that RCS enhanced the formation of N-DBPs much more than $HO^{\cdot}$. A previous study reported that $HO^{\cdot}$ can decrease the formation of N-DBPs in post-chlorination after the UV/H_2O_2 treatment of filtered drinking water (Chu et al., 2015). Therefore, the enhancement in N-DBP formation after the UV/chlorine treatment could be attributed to RCS. In addition, the UV photolysis of inorganic precursors (e.g., nitrite and nitrate) can result in the formation of RNS (Eqs. 1 and (2) (Lyon et al., 2012), which might have contributed to the increased formation of some N-DBPs in post-chlorination.

$$NO_3^- + hv \rightarrow NO_2^{\bullet} + O^{\bullet -} \quad (1)$$

$$NO_2^- + hv \rightarrow NO^{\bullet} + O^{\bullet -} \quad (2)$$

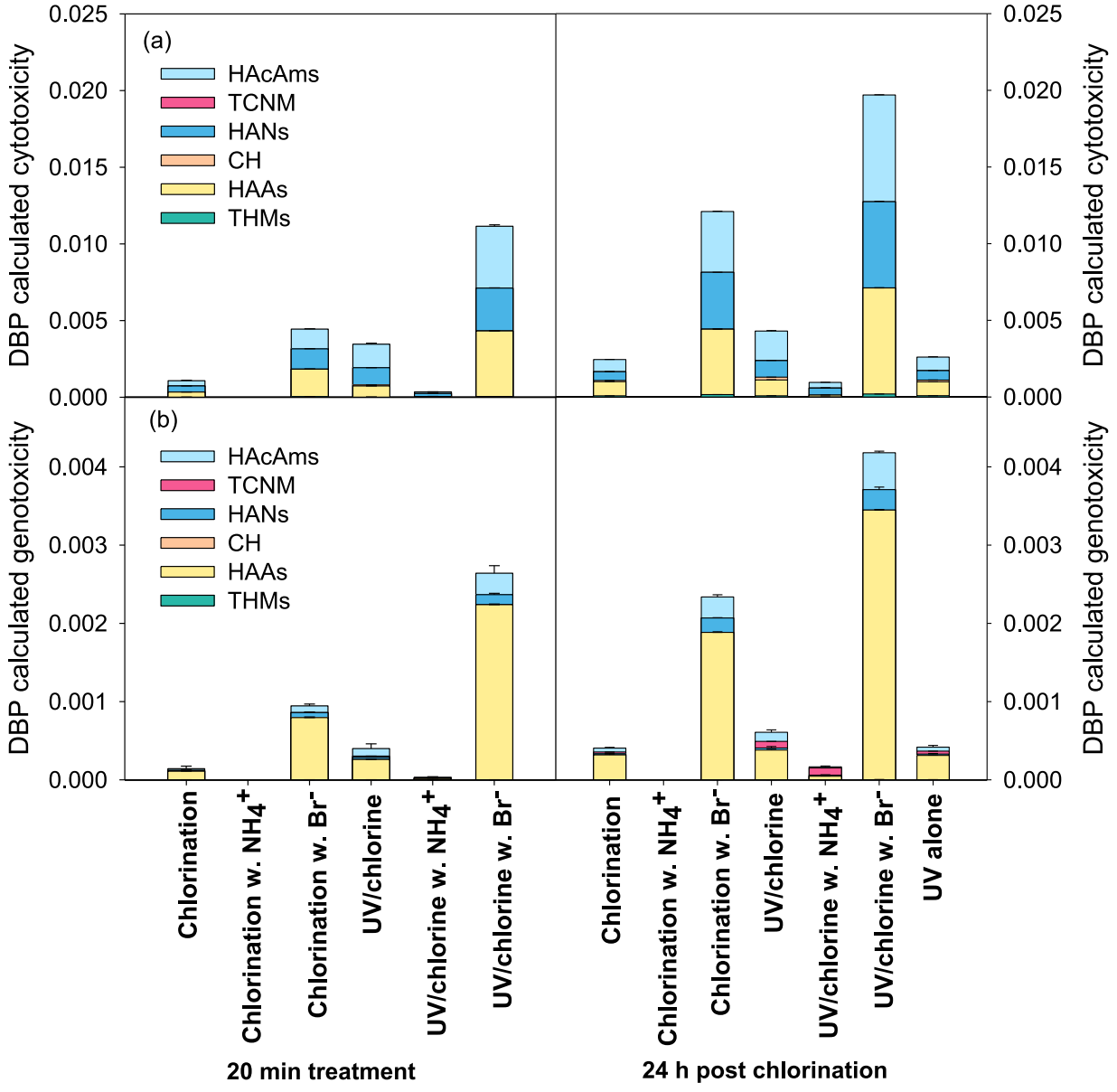

Fig. 3. Calculated cytotoxicity (a) and genotoxicity (b) of the DBPs during UV, chlorination and UV/chlorine treatments with or without additional ammonia and bromide, and 24 h post chlorination of wastewater. Conditions: [chlorine] = 200 μM, [NH_4^+] = 200 μM, [Br^-] = 1 mg/L, pH = 7.7.

3.1.3. Toxicity alteration in UV/chlorine-treated wastewater

Fig. 3 shows the calculated cytotoxicity and genotoxicity of the DBPs during the 20 min UV/chlorine treatment and 24 h post-chlorination. Cytotoxicity and genotoxicity of the DBPs are the chronic toxicity that inhibits cell growth and the acute toxicity that damages genomic DNA, respectively (Wagner and Plewa, 2017). The calculated cytotoxicity and genotoxicity of the DBPs in the UV/chlorine process were 2.2 and 2.8 times, respectively, those after chlorination alone. Of these, HAAs, HANs and HAcAms contributed to over 90% of the calculated cytotoxicity of both chlorination and the UV/chlorine treatment. HAAs contributed more than 65% of the highest genotoxicity, primarily due to the high genotoxicity of MBAA. During 24 h post-chlorination, the calculated DBP cytotoxicity and genotoxicity after the UV/chlorine treatment were 79% and 50%, respectively, higher than those after chlorination alone, due to the increased formation of HAAs, HANs and HAcAms.

Fig. 4 shows the changes in the acute toxicity and genotoxicity of organic extracts in the wastewater after 20 min chlorination, UV photolysis and UV/chlorine treatments. The acute toxicity and genotoxicity are comprehensive assessments of toxic organic compounds other than DBPs. The equivalent acute toxicity to *Vibrio fischeri* and genotoxicity of untreated wastewater determined by the *umu* test were 0.75 mg 3,5-DCP/L and 1.54 μg 4-NQO/L. Chlorination alone and UV photolysis of the wastewater slightly increased the acute toxicity by 12% and 9%, respectively, whereas the UV/chlorine treatment decreased the acute toxicity by 19%. The genotoxicity decreased by 30%, 39% and 76% after 20 min chlorination, UV and UV/chlorine treatments, respectively ($P < 0.05$).

Toxicity alteration in wastewater depends on the degradation of existing toxic substances during the treatment and the formation of new toxic transformation products. The transformation products formed during chlorination exhibited higher acute toxicity, leading to an increase in the acute toxicity of the wastewater. The acute toxicity was lower after the UV/chlorine treatment of trimethoprim than after chlorination, because $HO^{\cdot}$ and RCS decreased the acute toxicity (Wu et al., 2016). RCS not only formed toxic chlorinated

Table 2
Simulated concentrations of $HO^{\cdot}$ and reactive chlorine species in the UV/chlorine and UV/H_2O_2 processes at oxidant dosage of 200 μM and pH 7.7.

	$HO^{\cdot}$ (M)	$Cl^{\cdot}$ (M)	$ClO^{\cdot}$ (M)	$Cl_2^{\cdot-}$ (M)
UV/chlorine	6.78×10^{-14}	1.01×10^{-14}	1.77×10^{-12}	7.79×10^{-13}
UV/chlorine w. 200 μM ammonia	7.71×10^{-14}	3.67×10^{-14}	2.30×10^{-13}	2.89×10^{-12}
UV/chlorine w. 1 mg/L bromide	7.98×10^{-14}	9.00×10^{-15}	1.64×10^{-12}	5.96×10^{-13}
UV/H_2O_2	5.64×10^{-13}	3.99×10^{-19}	–	2.60×10^{-17}
Simulated concentrations of reactive bromine species in the UV/chlorine process at oxidant dosage of 200 μM and pH 7.7.				
	$Br^{\cdot}$ (M)	$Br_2^{\cdot-}$ (M)	$BrO^{\cdot}$ (M)	$BrCl^{\cdot-}$ (M)
UV/chlorine	3.45×10^{-15}	3.22×10^{-15}	2.24×10^{-11}	1.71×10^{-14}
UV/chlorine w. 1 mg/L bromide	7.28×10^{-14}	1.56×10^{-12}	2.47×10^{-10}	2.86×10^{-13}

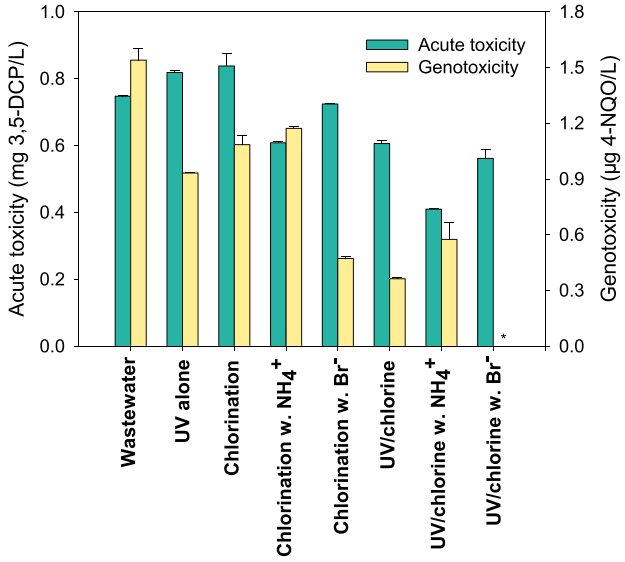

Fig. 4. Alteration of acute toxicity and genotoxicity of organic substances in wastewater treated by UV, chlorination, UV/chlorine with or without additional ammonia and bromide. * represents under the limit of detection. Conditions: [chlorine] = 200 μM, [NH_4^+] = 200 μM, [Br^-] = 1 mg/L, pH = 7.7.

products, but also tended to reduce the acute toxicity when degrading target pollutants (Shu et al., 2014; Wu et al., 2016). Chlorination and UV photolysis can eliminate some genotoxic materials in wastewater (Wu et al., 2012; Huang et al., 2019). $HO^{\cdot}$ and RCS further eliminated genotoxic materials in the wastewater during the UV/chlorine treatment. $CO_3^{\cdot-}$ could also decrease the genotoxicity of some organic compounds (Zhou et al., 2020). Hence, the UV/chlorine treatment efficiently degraded diverse organic compounds and simultaneously decreased the acute toxicity and genotoxicity of the wastewater.

3.2. Effects of ammonia on EfOM characterization, DBP formation and toxicity alteration in UV/chlorine-treated wastewater

The initial ammonia concentration of the wastewater was 0.04 mgN/L (3 μM). Additional 200 μM ammonia was added in the wastewater firstly before spiking free chlorine to simulate the wastewater with high concentration ammonia. The addition of 200 μM ammonia to the wastewater significantly decreased the removal efficiencies of fluorescent components and UVA_{254} by 37 – 43% and 26%, respectively ($P < 0.05$), in the UV/chlorine process (Fig. 1). The additional 200 μM ammonia completely converted chlorine into monochloramine when the chlorine dosage was 200 μM, which could mimic the application of a UV/chlorine treatment to wastewater with high ammonia levels or UV/monochloramine treatment. Monochloramine is a weak oxidant with a much lower degradation efficiency of organic compounds than free chlorine. According to the kinetic model, the steady state concentrations of $HO^{\cdot}$, $Cl^{\cdot}$ and $Cl_2^{\cdot-}$ increased by 14%, 2.6 times and 2.7 times, respectively, whereas that of $ClO^{\cdot}$ decreased by 87% during UV/chlorine treatment of wastewater with 200 μM ammonia (Table 2). $ClO^{\cdot}$ was primarily generated from the reaction of free chlorine ($HOCl/OCl^-$) with $HO^{\cdot}$ and $Cl^{\cdot}$. The conversion of free chlorine to monochloramine led to the significant decrease of $ClO^{\cdot}$. As previously mentioned, of the radicals in the UV/chlorine process, $ClO^{\cdot}$ was responsible for the degradation of EfOM. The conversion of free chlorine to chloramine led to decreases in $ClO^{\cdot}$ and the removal efficiencies of fluorescent components and aromaticity.

The formation of all the DBPs decreased considerably by 64 – 97% during 20 min UV/chlorine treatment of wastewater with 200 μM ammonia (Fig. 2). During the 24 h post-treatment, the formation of C-DBPs, HANs and HAcAms decreased by 88 – 98%, 66% and 43%, respectively, whereas that of TCNM increased by 11% ($P < 0.05$).

Monochloramine had a lower reactivity towards EfOM to form C-DBPs. The photolysis of monochloramine can generate reactive nitrate species (RNS), such as $NO^{\cdot}$ and $NO_2^{\cdot}$, according to eqs. 3-5 (Sun et al., 2019; Wu et al., 2019). Also, nitrite is the inorganic product of chloramine photolysis (De Laat et al., 2010) and can consume $HO^{\cdot}$ and $Cl^{\cdot}$ to form $NO_2^{\cdot}$ (Bu et al., 2020). The formation of RNS is likely to yield nitrogenous by-products, especially nitro products, which can act as TCNM precursors. Hence, the TCNM formation potential increased when ammonia was added to the UV/chlorine treatment.

$$NH_2^{\bullet} + O_2 \rightarrow NH_2O_2^{\bullet} \quad (3)$$

$$NH_2O_2^{\bullet} \rightarrow NO^{\bullet} + H_2O \quad (4)$$

$$2NO^{\bullet} + O_2 \rightarrow 2NO_2^{\bullet} \quad (5)$$

During the UV/chlorine treatment and 24 h post-chlorination with additional ammonia, the calculated DBP cytotoxicity decreased substantially by 90% and 78%, respectively, whereas the calculated DBP genotoxicity decreased by 92% and 73%, respectively (Fig. 3). HANs and HAcAms accounted for more than 85% of the cytotoxicity during the UV/chlorine treatment of wastewater with additional ammonia, whereas HAAs and TCNM were responsible for more than 82% of the genotoxicity. The acute toxicity and genotoxicity of the wastewater decreased to 0.41 mg 3,5-DCP/L and 0.58 μg 4-NQO/L, respectively, after the UV/chlorine treatment with additional ammonia (Fig. 4). The acute toxicity of wastewater spiked with 200 μM ammonia was 32% lower than that of unspiked wastewater after the UV/chlorine treatment, but the genotoxicity was 58% higher ($P < 0.05$). Chloramination alone de-

creased the acute toxicity of the wastewater, whereas chlorination increased it. The decrease in $ClO^{\cdot}$ led to a reduced removal efficiency of genotoxic materials. Meanwhile, nitrosated and nitrated products, which are expected to be more genotoxic (Chen et al., 2020), could form in the UV/monochloramine process (Wu et al., 2019).

3.3. Effects of bromide on EfOM characterization, DBP formation and toxicity alteration in UV/chlorine-treated wastewater

The initial bromide concentration in the wastewater was 40 μg/L (0.5 μM). The degradation of different fluorescent components and the reduction in UVA_{254} were slightly different for the UV/chlorine processes without and with additional 1 mg/L (12.5 μM) bromide (Fig. 1). With the additional 1 mg/L bromide, the concentration of $HO^{\cdot}$ increased slightly by 18%, whereas the concentrations of RCS decreased by 8 – 24% (Table 2). On the other hand, the concentrations of $Br^{\cdot}$, $Br_2^{\cdot-}$ and $BrCl^{\cdot-}$ increased by 1 – 3 orders of magnitude to 7.28×10^{-14} M, 1.56×10^{-12} M and 2.86×10^{-13} M, respectively, in the UV/chlorine process. Reactive bromine species (RBS) can attack organic compounds via electron transfer and hydrogen abstraction with rate constants in the range of 10^5 – 10^{10} M^{-1} s^{-1} (Guo et al., 2020; NIST, 2020). Therefore, the degradation rates of diverse components barely changed in the UV/chlorine process with additional bromide.

Compared with the UV/chlorine treatment without bromide addition, the UV/chlorine process with 1 mg/L bromide resulted in an increase in the formation of THMs by 86%, but decreases in the HAAs by 24%, HANs by 31% and HAcAms by 27% (Fig. 2) ($P < 0.05$). Additional bromide led to an increases of 122% and 36% in the formation of THMs and HANs, respectively, relative to the results obtained for post-chlorination preceded by the UV/chlorine treatment, whereas the formation of HAAs and HAcAms decreased by 24% and 14%, respectively.

The formation of bromine and RBS in the UV/chlorine process significantly increased the formation of brominated DBPs. Bromine tends to react with organic matter by substitution, but chlorine tends to cleave carbon bonds (Westerhoff et al., 2004). Bromine preferred to react with humic acid (C1) and fulvic acid (C2), which were reported to play a greater role in the formation of THMs than chlorine (Richardson et al., 2003). The presence of bromide in the UV/chlorine process can further produce organic matter with lower MWs (Zhao et al., 2011), providing more precursors of THMs. Bromine reacted with DOM via electrophilic substitution by lower than 40% to form brominated DBPs, while the remaining reaction occurred via electron transfer to form bromide (Langsa et al., 2017). The released bromide was recycled by chlorine to form bromine, resulting in further electrophilic substitution to generate more brominated DBPs. Compared with the 20 min chlorination with additional bromide, the UV/chlorine treatment led to a significant increase in the formation of bromo-DBPs and bromochloro-DBPs. The degree of bromination is often indicated by the bromine incorporation factor (BIF), which is defined as follows:

$$BIF_{THMs} = \frac{\sum_{n=1}^{3} n \times CHCl_{(3-n)}Br_n}{\text{Total THMs}} \quad (6)$$

$$BIF_{HAAs} = \frac{\sum_{n=1}^{3}\sum_{m=1}^{4-n} n \times C_2H_mO_2Cl_{(4-m-n)}Br_n}{\text{Total HAAs}} \quad (7)$$

$$BIF_{HANs} = \frac{\sum_{n=1}^{2} n \times C_2HNCl_{(2-n)}Br_n}{\text{Total HANs}} \quad (8)$$

$$BIF_{HAcAms} = \frac{\sum_{n=1}^{2} n \times C_2H_3NOCl_{(2-n)}Br_n + C_2H_2NOCl_2Br}{\text{Total HAcAms}} \quad (9)$$

The BIFs of the THMs, HAAs, HANs and HAcAms during the 20 min chlorination treatment with additional bromide were 61%, 48%, 45% and 48%, respectively, whereas they increased to 62%, 59%, 47% and 76%, respectively, during the UV/chlorine treatment with additional bromide.

The additional bromide significantly increased the calculated DBP cytotoxicity and genotoxicity by 2 – 6 times during the 20 min UV/chlorine treatment and subsequent 24 h chlorination. The brominated DBPs exhibited much higher cytotoxicity and genotoxicity to CHO cells than the chlorinated DBPs (Wagner and Plewa, 2017). With the additional bromide, the acute toxicity of the wastewater decreased to 0.56 mg 3,5- DCP/L, which was 7% lower than that during the UV/chlorine treatment without additional bromide ($P > 0.05$). The genotoxicity of the wastewater decreased to less than the limit of detection ($P < 0.05$). The genotoxicity of wastewater is responsible for some genotoxic materials that exist in wastewater, such as ofloxacin (Wu et al., 2010). The removal efficiency of genotoxic materials was higher during chlorination with bromide than during chlorination without bromide, as determined by *umu* tests (Wu et al., 2010). RBS could further decrease the genotoxic materials. Despite the increase in brominated DBPs, the presence of bromide during the UV/chlorine treatment efficiently eliminated toxic organic fractions from the wastewater.

4. Conclusions and engineering implications

This study investigated DBP formation and toxicity alteration in wastewater after UV/chlorine treatment and examined the effects of ammonia and bromide. RCS accelerated the degradation of components in the wastewater, but DBP formation increased during the UV/chlorine treatment. However, compared with chlorination alone, the UV/chlorine treatment reduced the acute toxicity and genotoxicity of organic matter in the wastewater. The addition of 200 μM ammonia decreased the concentration of $ClO^{\cdot}$ but increased the concentrations of $HO^{\cdot}$, $Cl^{\cdot}$ and $Cl_2^{\cdot-}$ in the UV/chlorine process, which decreased the removal efficiency of organic substances from the wastewater; however, compared with the UV/chlorine treatment without ammonia, the addition of ammonia slightly decreased the acute toxicity and increased the genotoxicity of the wastewater. The high concentration of ammonia increased the formation of TCNM in post-chlorination after the UV/chlorine treatment. An additional 1 mg/L bromide in the UV/chlorine process led to the formation of bromine and RBS, which considerably increased the formation of brominated DBPs and the corresponding cytotoxicity and genotoxicity. However, the acute toxicity and genotoxicity of the wastewater were further decreased.

Compared with the traditional UV/H_2O_2 treatment, the UV/chlorine treatment exhibited a better performance in terms of the removal efficiency of organic components from the wastewater. The formation of THMs in post-chlorination after the UV/chlorine treatment was 18% lower than that after the UV/H_2O_2 treatment, whereas the formation of N-DBPs was 77 – 101% higher after the UV/chlorine treatment (Fig. S4). Ammonia and bromide are common ions in wastewater that affect the chlorine and radical chemistry in the UV/chlorine process and thus DBP and toxicity alteration. The trends in DBP formation and the calculated DBP cytotoxicity and genotoxicity were not consistent with those in the acute toxicity and mutability. More toxicity bioassays should be conducted to further evaluate the effects of the UV/chlorine treatment on wastewater quality.

Declaration of Competing Interest

The authors declare that they have no known competing financial interests or personal relationships that could have appeared to influence the work reported in this paper.

Acknowledgments

This work was financially supported by the Natural Science Foundation of China (21677181, 21922612, 51908564), the National Key Research Development Program of China (2016YFC0502803), and the Research Fund Program of Guangdong Key Laboratory of Environmental Catalysis and Health Risk Control (GKECHRC-01).

Supplementary materials

Supplementary material associated with this article can be found, in the online version, at doi:10.1016/j.watres.2020.116549.

References

Alfassi, Z.B., Huie, R.E., Mosseri, S., Neta, P., 1988. Kinetics of one-electron oxidation by the ClO radical. Radiat. Phys. Chem. 1, 85–88.
APHA-AWWA-WEF, 2012. Standard methods for the examination of water and wastewater. 22nd, American Public Health Association/American Water Works Association/Water Environment Federation.
Baxendale, J.H., Wilson, J.A., 1957. The photolysis of hydrogen peroxide at high light intensities. Trans. Faraday Soc. 53, 344–356.
Bolton, J.R., Stefan, M.I., Shaw, P., Lykke, K.R., 2011. Determination of the quantum yields of the potassium ferrioxalate and potassium iodide–iodate actinometers and a method for the calibration of radiometer detectors. J. Photochem. Photobiol. A 222, 166–169.
Brigante, M., Minella, M., Mailhot, G., Maurino, V., Minero, C., Vione, D., 2014. Formation and reactivity of the dichloride radical (Cl_2-) in surface waters: A modelling approach. Chemosphere 95, 464–469.
Bu, L., Sun, J., Wu, Y., Zhang, W., Duan, X., Zhou, S., Dionysiou, D.D., Crittenden, J.C., 2020. Non-negligible risk of chloropicrin formation during chlorination with the UV/persulfate pretreatment process in the presence of low concentrations of nitrite. Water Res. 168, 115194.
Bulman, D., Remucal, C.K., 2020. The role of reactive halogen species in disinfection by-product formation during chlorine photolysis. Environ. Sci. Technol. 54, 9629–9639.
Chen, C., Wu, Z., Zheng, S., Wang, L., Niu, X., Fang, J., 2020. Comparative study for interactions of sulfate radical and hydroxyl radical with phenol in the presence of nitrite. Environ. Sci. Technol. 54, 8455–8463.
Chen, W., Westerhoff, P., Leenheer, J.A., Booksh, K., 2003. Fluorescence excitation−emission matrix regional integration to quantify spectra for dissolved organic matter. Environ. Sci. Technol. 37, 5701–5710.
Cheng, S., Zhang, X., Yang, X., Shang, C., Song, W., Fang, J., Pan, Y., 2018. The multiple role of bromide ion in PPCPs degradation under UV/chlorine treatment. Environ. Sci. Technol. 52, 1806–1816.
Chu, W., Li, D., Gao, N., Templeton, M.R., Tan, C., Gao, Y., 2015. The control of emerging haloacetamide DBP precursors with UV/persulfate treatment. Water Res 72, 340–348.
Chuang, Y., Chen, S., Chinn, C.J., Mitch, W.A., 2017. Comparing the UV/monochloramine and UV/free chlorine advanced oxidation processes (AOPs) to the UV/hydrogen peroxide AOP under scenarios relevant to potable reuse. Environ. Sci. Technol. 51, 13859–13868.
Chuang, Y., Szczuka, A., Shabani, F., Munoz, J., Aflaki, R., Hammond, S.D., Mitch, W.A., 2019. Pilot-scale comparison of microfiltration/reverse osmosis and ozone/biological activated carbon with UV/hydrogen peroxide or UV/free chlorine AOP treatment for controlling disinfection byproducts during wastewater reuse. Water Res. 152, 215–225.
De Laat, J., Boudiaf, N., Dossier-Berne, F., 2010. Effect of dissolved oxygen on the photodecomposition of monochloramine and dichloramine in aqueous solution by UV irradiation at 253.7 nm. Water Res. 44, 3261–3269.
Deng, L., Huang, C., Wang, Y., 2014. Effects of combined UV and chlorine treatment on the formation of trichloronitromethane from amine precursors. Environ. Sci. Technol. 48, 2697–2705.
Fang, J., Fu, Y., Shang, C., 2014. The roles of reactive species in micropollutant degradation in the UV/free chlorine system. Environ. Sci. Technol. 48, 1859–1868.
Gao, Z., Lin, Y., Xu, B., Xia, Y., Hu, C., Zhang, T., Cao, T., Chu, W., Gao, N., 2019. Effect of UV wavelength on humic acid degradation and disinfection by-product formation during the UV/chlorine process. Water Res. 154, 199–209.
Gao, Z., Lin, Y., Xu, B., Xia, Y., Hu, C., Zhang, T., Qian, H., Cao, T., Gao, N., 2020. Effect of bromide and iodide on halogenated by-product formation from different organic precursors during UV/chlorine processes. Water Res. 182, 116035.
Guo, K., Wu, Z., Shang, C., Yao, B., Hou, S., Yang, X., Song, W., Fang, J., 2017. Radical chemistry and structural relationships of PPCP degradation by UV/chlorine treatment in simulated drinking water. Environ. Sci. Technol. 51, 10431–10439.
Guo, K., Wu, Z., Yan, S., Yao, B., Song, W., Hua, Z., Zhang, X., Kong, X., Li, X., Fang, J., 2018. Comparison of the UV/chlorine and UV/H_2O_2 processes in the degradation of PPCPs in simulated drinking water and wastewater: kinetics, radical mechanism and energy requirements. Water Res. 147, 184–194.
Guo, K., Zheng, S., Zhang, X., Zhao, L., Ji, S., Chen, C., Wu, Z., Wang, D., Fang, J., 2020. Roles of bromine radicals and hydroxyl radicals in the degradation of micropollutants by the UV/Bromine process. Environ. Sci. Technol. 54, 6415–6426.
Hua, Z., Guo, K., Kong, X., Lin, S., Wu, Z., Wang, L., Huang, H., Fang, J., 2019a. PPCP degradation and DBP formation in the solar/free chlorine system: effects of pH and dissolved oxygen. Water Res. 150, 77–85.
Hua, Z., Kong, X., Hou, S., Zou, S., Xu, X., Huang, H., Fang, J., 2019b. DBP alteration from NOM and model compounds after UV/persulfate treatment with post chlorination. Water Res 158, 237–245.
Huang, H., Chen, B., Zhu, Z., 2017. Formation and speciation of haloacetamides and haloacetonitriles for chlorination, chloramination, and chlorination followed by chloramination. Chemosphere 166, 126–134.
Huang, W., Du, Y., Liu, M., Hu, H., Wu, Q., Chen, Y., 2019. Influence of UV irradiation on the toxicity of chlorinated water to mammalian cells: Toxicity drivers, toxicity changes and toxicity surrogates. Water Res. 165, 115024.
Hwang, C.J., Krasner, S.W., Krasner, S.W., Sclimenti, M.J., Amy, G.L., Dickenson, E., 2002. Polar NOM: characterization, DBPs, and treatment. Am. Water Works Assoc..
Ianni, J. C., 2015. Kintecus, www.kintecus.com.
Korshin, G.V., Kumke, M.U., Li, C., Frimmel, F.H., 1999. Influence of chlorination on chromophores and fluorophores in humic substances. Environ. Sci. Technol. 33, 1207–1212.
Lamsal, R., Walsh, M.E., Gagnon, G.A., 2011. Comparison of advanced oxidation processes for the removal of natural organic matter. Water Res. 45, 3263–3269.
Langsa, M., Heitz, A., Joll, C.A., von Gunten, U., Allard, S., 2017. Mechanistic aspects of the formation of adsorbable organic bromine during chlorination of bromide–containing synthetic waters. Environ. Sci. Technol. 51, 5146–5155.
Lei, Y., Cheng, S., Luo, N., Yang, X., An, T., 2019. Rate constants and mechanisms of the reactions of $Cl^{\cdot}$ and $Cl_2^{\cdot-}$ with trace organic contaminants. Environ. Sci. Technol. 53, 11170–11182.
Li, J., Blatchley III, E.R., 2009. UV photodegradation of inorganic chloramines. Environ. Sci. Technol. 43, 60–65.
Li, T., Jiang, Y., An, X., Liu, H., Hu, C., Qu, J., 2016. Transformation of humic acid and halogenated byproduct formation in UV-chlorine processes. Water Res. 102, 421–427.
Lv, X., Zhang, X., Du, Y., Wu, Q., Lu, Y., Hu, H., 2017. Solar light irradiation significantly reduced cytotoxicity and disinfection byproducts in chlorinated reclaimed water. Water Res. 125, 162–169.
Lyon, B.A., Dotson, A.D., Linden, K.G., Weinberg, H.S., 2012. The effect of inorganic precursors on disinfection byproduct formation during UV-chlorine/chloramine drinking water treatment. Water Res. 46, 4653–4664.
Ma, H., Allen, H.E., Yin, Y., 2001. Characterization of isolated fractions of dissolved organic matter from natural waters and a wastewater effluent. Water Res. 35, 985–996.
Magazinovic, R.S., Nicholson, B.C., Mulcahy, D.E., Davey, D.E., 2004. Bromide levels in natural waters: Its relationship to levels of both chloride and total dissolved solids and the implications for water treatment. Chemosphere 57, 329–335.
Miklos, D.B., Wang, W.L., Linden, K.G., Drewes, J.E., Hübner, U., 2019. Comparison of UV-AOPs (UV/H_2O_2, UV/PDS and UV/Chlorine) for TOrC removal from municipal wastewater effluent and optical surrogate model evaluation. Chem. Eng. J. 362, 537–547.
Muellner, M.G., Wagner, E.D., McCalla, K., Richardson, S.D., Woo, Y., Plewa, M.J., 2007. Haloacetonitriles vs. Regulated haloacetic acids: are nitrogen-containing DBPs more toxic? Environ. Sci. Technol. 41, 645–651.
Murphy, K.R., Stedmon, C.A., Graeber, D., Bro, R., 2013. Fluorescence spectroscopy and multi-way techniques. PARAFAC. Anal. Methods. 5, 6557–6566 .
National institute of standards and technology. NDRL/NIST solution kinetics database on the web. Http://www3.nd.edu/~ndrlrcdc/index.html (Accessed March 29, 2020).
Parvez, S., Venkataraman, C., Mukherji, S., 2006. A review on advantages of implementing luminescence inhibition test (Vibrio fischeri) for acute toxicity prediction of chemicals. Environ. Int. 32, 265–268.
Pisarenko, A.N., Stanford, B.D., Snyder, S.A., Rivera, S.B., Boal, A.K., 2013. Investigation of the use of chlorine based advanced oxidation in surface water: oxidation of natural organic matter and formation of disinfection byproducts. J. Adv. Oxid. Technol. 16, 137–145.
Plewa, M.J., Wagner, E.D., Jazwierska, P., Richardson, S.D., Chen, P.H., McKague, A.B., 2004. Halonitromethane drinking water disinfection byproducts: chemical characterization and mammalian cell cytotoxicity and genotoxicity. Environ. Sci. Technol. 38, 62–68.
Plewa, M.J., Wagner, E.D., Metz, D.H., Kashinkunti, R., Jamriska, K.J., Meyer, M., 2012. Differential toxicity of drinking water disinfected with combinations of ultraviolet radiation and chlorine. Environ. Sci. Technol. 46, 7811–7817.
Reckhow, D.A., MacNeill, A.L., Platt, T.L., MacNeill, A.L., McClellan, J.N., 2001. Formation and degradation of dichloroacetonitrile in drinking waters. J. Water Supply Res. T. 50, 1–13.
Reifferscheid, G., Heil, J., 1996. Validation of the SOS/ umu test results of 486 chemicals and comparison with the Ames test and carcinogenicity data. Mutat. Res. 369, 129.
Remucal, C.K., Manley, D., 2016. Emerging investigators series: The efficacy of chlorine photolysis as an advanced oxidation process for drinking water treatment. Environ. Sci.: Water Res. Technol. 2, 565–579.

Richardson, S.D., Thruston, A.D., Rav-Acha, C., Groisman, L., Popilevsky, I., Juraev, O., Glezer, V., McKague, A.B., Plewa, M.J., Wagner, E.D., 2003. Tribromopyrrole, brominated acids, and other disinfection byproducts produced by disinfection of drinking water rich in bromide. Environ. Sci. Technol. 37, 3782–3793.
Shu, Z., Li, C., Belosevic, M., Bolton, J.R., El-Din, M.G., 2014. Application of a solar UV/chlorine advanced oxidation process to oil sands process-affected water remediation. Environ. Sci. Technol. 48, 9692–9701.
Sichel, C., Garcia, C., Andre, K., 2011. Feasibility studies: UV/chlorine advanced oxidation treatment for the removal of emerging contaminants. Water Res. 45, 6371–6380.
Soltermann, F., Abegglen, C., Götz, C., von Gunten, U., 2016. Bromide sources and loads in swiss surface waters and their relevance for bromate formation during wastewater ozonation. Environ. Sci. Technol. 50, 9825–9834.
Sun, P., Meng, T., Wang, Z., Zhang, R., Yao, H., Yang, Y., Zhao, L., 2019. Degradation of organic micropollutants in UV/NH_2Cl advanced oxidation process. Environ. Sci. Technol. 53, 9024–9033.
Sun, Y., Wu, Q., Hu, H., Tian, J., 2009. Effect of bromide on the formation of disinfection by-products during wastewater chlorination. Water Res. 43, 2391–2398.
USEPA, 1995. Method 551.1: Determination of chlorination disinfection byproducts, chlorinated solvents, and halogenated pesticides/herbicides in drinking water by liquid-liquid extraction and gas chromatography with electron-capture detection. American Public Health Assoc, Washington. DC. USA Revision 1.0.
USEPA, 2003. Method 552.3: Determination of haloacetic acids and dalapon in drinking water by liquid-liquid microextraction, derivatization, and gas chromatography with electron capture detection. American Public Health Assoc, Washington. DC. USA Revision 1.0.
Wagner, E.D., Plewa, M.J., 2017. CHO cell cytotoxicity and genotoxicity analyses of disinfection by-products: an updated review. J. Environ. Sci. 58, 64–76.
Wang, C., Moore, N., Bircher, K., Andrews, S., Hofmann, R., 2019. Full-scale comparison of UV/H_2O_2 and UV/Cl_2 advanced oxidation: the degradation of micropollutant surrogates and the formation of disinfection byproducts. Water Res. 161, 448–458.
Wang, D., Bolton, J.R., Andrews, S.A., Hofmann, R., 2015. Formation of disinfection by-products in the ultraviolet/chlorine advanced oxidation process. Sci. Total Environ. 518-519, 49–57.
Wang, W., Zhang, X., Wu, Q., Du, Y., Hu, H., 2017. Degradation of natural organic matter by UV/chlorine oxidation: molecular decomposition, formation of oxidation byproducts and cytotoxicity. Water Res. 124, 251–258.
Westerhoff, P., Chao, P., Mash, H., 2004. Reactivity of natural organic matter with aqueous chlorine and bromine. Water Res. 38, 1502–1513.
Wu, D., Zhang, F., Lou, W., Li, D., Chen, J., 2017a. Chemical characterization and toxicity assessment of fine particulate matters emitted from the combustion of petrol and diesel fuels. Sci. Total Environ. 605-606, 172–179.
Wu, Q., Li, Y., Hu, H., Ding, Y., Huang, H., Zhao, F., 2012. Removal of genotoxicity in chlorinated secondary effluent of a domestic wastewater treatment plant during dechlorination. Environ. Sci. Pollut. R. 19, 1–7.
Wu, Q., Li, Y., Hu, H., Sun, Y., Zhao, F., 2010. Reduced effect of bromide on the genotoxicity in secondary effluent of a municipal wastewater treatment plant during chlorination. Environ. Sci. Technol. 44, 4924–4929.
Wu, Z., Chen, C., Zhu, B., Huang, C., An, T., Meng, F., Fang, J., 2019. Reactive nitrogen species are also involved in the transformation of micropollutants by the UV/monochloramine process. Environ. Sci. Technol. 19, 11142–11152.
Wu, Z., Fang, J., Xiang, Y., Shang, C., Li, X., Meng, F., Yang, X., 2016. Roles of reactive chlorine species in trimethoprim degradation in the UV/chlorine process: kinetics and transformation pathways. Water Res. 104, 272–282.
Wu, Z., Guo, K., Fang, J., Yang, X., Xiao, H., Hou, S., Kong, X., Shang, C., Yang, X., Meng, F., Chen, L., 2017b. Factors affecting the roles of reactive species in the degradation of micropollutants by the UV/chlorine process. Water Res. 126, 351–360.
Xie, P., Ma, J., Liu, W., Zou, J., Yue, S., 2015. Impact of UV/persulfate pretreatment on the formation of disinfection byproducts during subsequent chlorination of natural organic matter. Chem. Eng. J. 269, 203–211.
Yan, S., Liu, Y., Lian, L., Li, R., Ma, J., Zhou, H., Song, W., 2019. Photochemical formation of carbonate radical and its reaction with dissolved organic matters. Water Res. 161, 288–296.
Yang, Y., Pignatello, J.J., Ma, J., Mitch, W.A., 2016. Effect of matrix components on UV/H_2O_2 and UV/$S_2O_8^{2-}$ advanced oxidation processes for trace organic degradation in reverse osmosis brines from municipal wastewater reuse facilities. Water Res. 89, 192–200.
Zhao, Q., Shang, C., Zhang, X., Ding, G., Yang, X., 2011. Formation of halogenated organic byproducts during medium-pressure UV and chlorine coexposure of model compounds. NOM and bromide. Water Res. 45, 6545–6554.
Zhou, Y., Chen, C., Guo, K., Wu, Z., Wang, L., Hua, Z., Fang, J., 2020. Kinetics and pathways of the degradation of PPCPs by carbonate radicals in advanced oxidation processes. Water Res. 185, 116231.
Zhong, Y., Gan, W., Du, Y., Huang, H., Wu, Q., Xiang, Y., Shang, C., Yang, X., 2019. Disinfection byproducts and their toxicity in wastewater effluents treated by the mixing oxidant of ClO_2/Cl_2. Water Res. 162, 471–481.